Interpreting epidemiological surveillance data: A modelling study based on Pune City

Prathith Bhargav[1☯*], Soumil Kelkar[1☯], Joy Merwin Monteiro[2,3], Philip Cherian[4],

1 Indian Institute of Science Education and Research Pune, Dr Homi Bhabha Road, Pashan, Pune, Maharashtra - 411008 INDIA.

2 Department of Earth and Climate Science, Indian Institute of Science Education and Research Pune, Dr Homi Bhabha Road, Pashan, Pune, Maharashtra - 411008 INDIA.

3 Department of Data Science, Indian Institute of Science Education and Research Pune, Dr Homi Bhabha Road, Pashan, Pune, Maharashtra - 411008 INDIA.

4 Department of Physics, Ashoka University, Plot No. 2, Rajiv Gandhi Education City, Rai, Sonepat, Haryana - 131029 INDIA.

☯These authors contributed equally to this work.

*Corresponding Author. Email: prathith.bhargav.iiser@gmail.com

Abstract

Routine epidemiological surveillance data represents one of the most continuous and current sources of data during the course of an epidemic. This data is used to calibrate epidemiological forecasting models as well as for public health decision making such as imposition and lifting of lockdowns and quarantine measures. However, such data is generated during testing and contact tracing and not through randomized sampling. Furthermore, since the process of generating this data affects the epidemic trajectory itself – identification of infected persons might lead to them being quarantined, for instance – it is unclear how representative such data is of the actual epidemic itself. For example, will the observed rise in infections correspond well with the actual rise in infections? To answer such questions, we employ epidemiological simulations *not to study the effectiveness of different public health strategies in controlling the spread of the*

epidemic, but to study the quality of the resulting surveillance data and derived metrics and their utility for decision making. Using the BharatSim simulation framework, we build an agent-based epidemiological model with a detailed representation of testing and contact tracing strategies based on those employed in Pune city during the COVID-19 pandemic. Infected persons are identified, quarantined and/or hospitalized based on these strategies, and to generate synthetic surveillance data as well. We perform extensive simulations to study the impact of different public health strategies and availability of tests and contact tracing efficiencies on the resulting surveillance data as well as on the course of the epidemic. The fidelity of the resulting surveillance data in representing the real-time state of the epidemic and in decision-making is explored in the context of Pune city.

Author Summary

Through this study, we evaluate the effectiveness of different public health metrics in guiding decision-making during epidemics, using the COVID-19 pandemic in Pune, India, as a case study. We analysed key public health metrics including the test positivity rate (TPR), case fatality rate (CFR), and reproduction number (R_t). Through simulations of the epidemic and the public health response and by varying levels of testing and contact tracing, we assess how these metrics are related to epidemic curves such as infections and deaths. The results show that the rate of change of TPR can help estimate the severity of the outbreak and predict when it will peak. R_t is a strong predictor of the infection peak, but large computed confidence intervals can place strong caveats on its use in decision-making. In contrast, CFR is not useful for predicting the epidemic's severity or peak,as it tends to peak when the infection curve is on a decline and scales non-linearly with the severity of the epidemic. Overall, our findings highlight that TPR and R_t are valuable tools for real-time epidemic management, while CFR may have limited utility. Through this study, we provide modelling evidence to support the use of some metrics for public-health decision making during epidemics.

1 Introduction

Routine epidemiological surveillance data is generated by public and private entities as part of efforts to diagnose, treat and contain any outbreak [1]. For instance, during COVID-19 outbreaks in Pune city, daily surveillance data [2] included (1) the number of tests conducted, (2) the number of individuals who tested positive and their demographic information, (3) the number of people hospitalised, (4) the number of deaths, and (5) contacts of identified positive cases. Such surveillance data has been used as input for several epidemiological forecasting models [3–9] which have tried to estimate the course of the epidemic in India. Even though these forecasting models have their merits in assisting decision-making and policies, they come with their own set of challenges [10–12]. Similarly, surveillance data represents a noisy estimate of the actual epidemic and therefore it is important to understand its limitations. Some analytical results have been obtained to model the introduction of delays and under-reporting [13], but it is unlikely that the complexities of the public health response itself, such as testing, contact tracing and quarantining as well and resource constraints (such as number of testing kits available) can be easily modelled in an analytical framework. Therefore, simulations appear to be a useful tool to help understand the relationship between surveillance data and the true epidemic.

In addition to forecast models, metrics derived from surveillance data such as Test Positivity Rate (TPR), Case Fatality Rate (CFR) and Reproduction Number (R_t) have themselves also been used to inform public health interventions. The World Health Organization (WHO) advocated the use of TPR as a metric to indicate whether the epidemic is controlled [14]. While this recommendation was not prescriptive or data-driven, India, like many other countries, used TPR to gauge the true extent of the pandemic and subsequently implement public health measures [15, 16]. All over India, different districts were demarcated into red, orange, or green zones [17, 18] based on indicators derived from programmatic surveillance, including the number of daily cases and the extent of testing and surveillance. Moreover, local governments implemented strategies such as large-scale random testing to reduce the value of metrics like TPR [19], hoping, in turn, to reduce the spread of the epidemic.

Even though such metrics provide useful insights into the nature of the true epidemic

[20], understanding the correspondence between the actual epidemic curve and such metrics alone remains a challenge. These indicators are often biased and may not pick up asymptomatic carriers of the disease or even symptomatic carriers who choose not to self-report due to social or economic reasons [21]. Moreover, practical issues like limited resources, accessibility, and errors in data collection or analysis can lead to undercounting [22, 23]. Evidence of such undercounting has been reported through the use of serological surveys [24, 25]. Thus, it is essential to understand the relationship between the true epidemic and the "observed" epidemic as inferred from surveillance data.

Towards this end, we build an agent-based epidemiological model using the BharatSim simulation framework [9] that simulates an epidemic and the attendant public health response in the form of testing, quarantining, and contact tracing. We build this model in the context of the public health system response to the COVID-19 pandemic in the city of Pune, India. Several epidemiological models already exist in literature [26–31] that simulate an epidemic by assigning different disease states to people throughout the course of the epidemic. We choose an agent-based approach since it allows us to specify characteristics such as geographical locations and activity schedules for each individual (See Appendix S1). Likewise, this approach also allows us to track each individual's disease state, testing and quarantining status, and identified contacts, throughout the pandemic. In addition to modelling the spread of the epidemic, we also consider counterfactual scenarios with different public health responses, thereby studying the relationship between derived metrics and the true epidemic.

1.1 COVID-19 in Pune city

Pune city is located in the state of Maharashtra in western peninsular India and has a current estimated population of 4.5 million. The smallest administrative units are the electoral wards or "prabhags", and Pune consists of 41 prabhags, each containing approximately 100,000 people.[1] These prabhags are part of a larger administrative unit called a "ward", and each ward has a health officer who makes operational decisions such as deploying personnel for contact tracing or disinfection.

[1] Recent expansion of the city to include suburbs has increased this number. See https://www.pmc.gov.in/en/pmc-prabhag-rachna-2022.

The first case of COVID-19 in Pune city was reported on March 9, 2020. Pune experienced three major waves of the pandemic – the first between May-September 2020, the second between February-May 2021 and the third between December 2021-January 2022 [32]. Pune experienced a complete lockdown between March-June 2020 and wards with a high number of cases were quarantined from the rest of the city. Despite these strict containment measures, the rate of growth of cases continued to increase [33] and very high prevalence was observed in an early serological survey [34], suggesting that the spread of SARS-CoV2 within containment zones was fairly unrestricted. The Infection Fatality Rate computed using serological prevalence was comparable to results obtained elsewhere in the world [34], suggesting that undercounting of COVID-19 related deaths in Pune city was not substantial. With improvements in treatment protocols, the case fatality rate in Pune declined almost monotonically between March 2020 and May 2021, though the burden of mortality was much higher in the second wave [35].

A compartmental epidemiological model (which also forms the basis for our model) was operationally deployed during the first and second waves and forecasts were used in infrastructure planning, especially for critical cases who required ventilator support [20, 36]. While lockdowns were the main policy instrument used during the first year of the pandemic, a more fine-grained policy for restriction of movement and economic activity based on oxygenated bed occupancy levels and test positivity were employed from June 2021, after the end of the second wave [37–39], with the explicit intention of reducing further spread or "breaking the chain". Surveillance data was also used in estimates of prevalence and decision-making, using heuristic ideas relating case fatality rate, test positivity to actual prevalence, and allocation of limited testing kits [20]. The use of epidemiological surveillance data for decision-making is not unique to Maharashtra, and has been attempted elsewhere as well see, for example [40–43]. In the next section, we describe our epidemiological model and how the public health response was incorporated into it. As a first step, we do not attempt to incorporate interventions such as lockdowns to keep the model simpler and results interpretable.

2 Materials and methods

2.1 Population Structure

We model a "Prabhag" of Pune City, consisting of 100,000 individuals. These individuals are distributed demographically based on the estimated population data for 2012-14 [44]. We allocate unique attributes to all individuals, including information related to their home, office and neighbourhood locations (See Appendix S1 for a detailed description). People "move" between these locations based on a schedule defined by their attributes. For instance, an "employee" (any individual with an age under 60 years) travels daily to their office in the morning, spends some time in their neighbourhood, and comes back home in the evening (A schematic of the same is shown in Fig. 1). For a detailed description of the schedules, see Appendix S1. We model an isolated prabhag with no movement of the infection across prabhag boundaries.

2.2 Modelling the Public Health Response

Our model for the public health response is based on interviews with officials at the Pune city COVID-19 "war-room", a central data-gathering hub during 2020-2022. We elicited information regarding strategies to identify individuals for testing, contact tracing and quarantine. Analysis of contact tracing data between March-June 2020 (see Appendix S6) suggested that on average, around seven contacts were identified for each index patient and contacts were designated as high or low-risk based on proximity and duration of contact (see following sections for more details).

While introducing testing, we consider scenarios where the start of the actual epidemic is not coincident with the start of the public health response. For instance, in India, while the first case of COVID-19 was detected in January 2020 [45], the availability of tests was limited until May 2020, when about 453 tests per million people became available [46]. To mimic this scenario, we activate testing only after a threshold number of people "self-report" themselves as being sick.

There are three possible interventions through which an individual becomes eligible for testing — Self-Reporting, Contact Tracing, and Random Testing. Depending on the public health response, some of these interventions may or may not be active. We assume

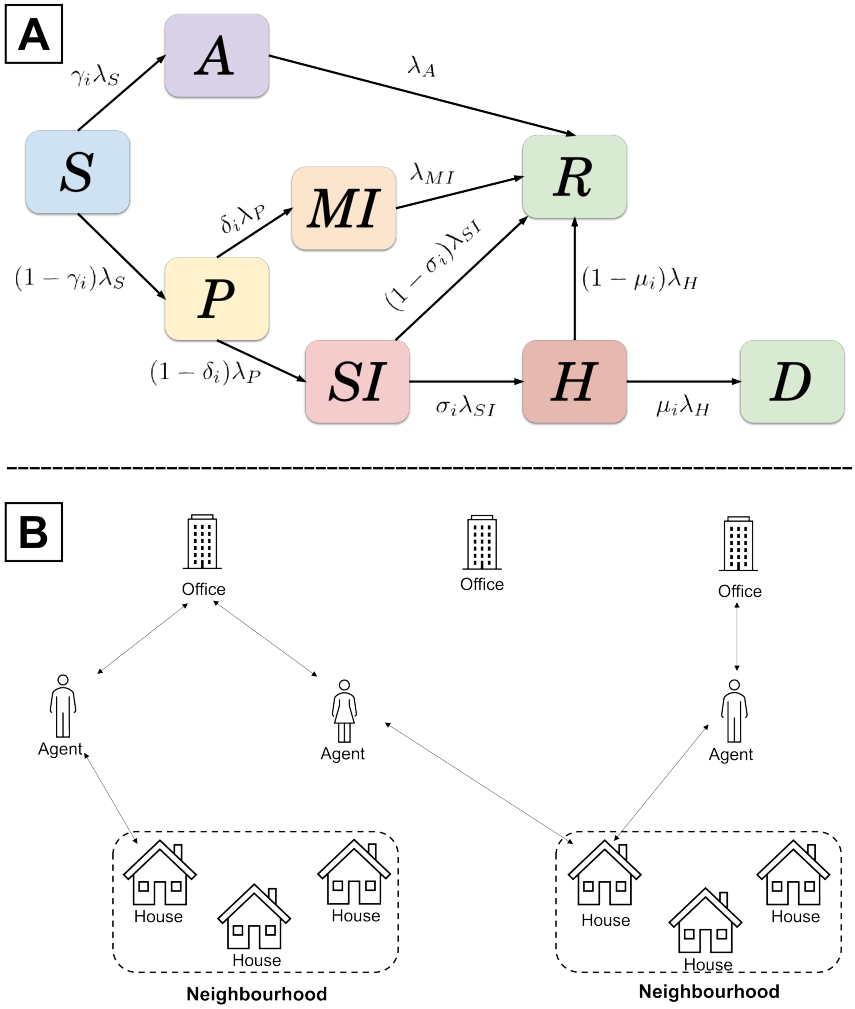

Fig 1. (A) A schematic describing the eight disease states and the transitions between them. (B) A schematic of the geographical structure depicting the movement of people between different locations. The agents (individuals) depicted here are employees who travel daily to their office, spend some time in their neighbourhood and come back home.

that there are limited tests every day and thus, not everyone who becomes eligible for getting a test is immediately tested. Depending on the number of tests, individuals are randomly selected from the list of all eligible people and are tested based on a priority order described below. Note that individuals who are eligible for getting tested are isolated until they receive their test.

Self-reporting Individuals exhibiting symptoms of COVID-19 can self-report and become eligible for receiving a test. Similar to real life, not all individuals will report their symptoms, and there is a probability associated with reporting symptoms. People with severe symptoms are more likely to self-report than people with mild symptoms. Moreover, not all people exhibiting symptoms are infected with COVID-19. During the epidemic, other diseases like the flu are still prevalent, and people infected with them exhibit similar symptoms [47]. To mimic this in our model, a small fraction of individuals (on average, 0.025% of the susceptible population) infected with flu-like illnesses (but still susceptible to COVID-19) report their symptoms every day and become eligible for getting a test. For simplicity, we assume that the people infected with or recovered from COVID-19 are not susceptible to other flu-like illnesses.

Contact tracing Contacts are individuals who might have interacted with an agent who tested positive. All individuals from the same household and a fraction of individuals belonging to the same office and the same neighbourhood as the agent who tested positive are selected as contacts. All household contacts (irrespective of their symptom status) and all symptomatic office and neighbourhood contacts are classified as high-risk contacts, and they are made eligible for testing. All the asymptomatic office and neighbourhood contacts are classified as low-risk contacts, and they are isolated for 7 days.

Random testing Individuals are randomly selected from the population and are made eligible for getting a test. These individuals are selected only if they are not already hospitalised or eligible for a test through any other interventions mentioned above. Moreover, positively tested, quarantined, or isolated individuals are also not selected.

Priority order for testing Even during the peak of the first wave of the epidemic, only about 12,000 tests were conducted daily in the Pune district, which is home to approximately 12 million people [48]. National statistics also paint a similar picture [49], and about a million tests were performed daily for a population of around 1.4 billion people. Considering the limited number of tests, the Indian Council of Medical Research formulated a set of guidelines to test individuals based on a priority order [50]. We simulate such guidelines with a limited number of daily tests and a priority order for

who receives the test. The priority order is as follows:

1. Self-reported symptomatic individuals and high-risk contacts
2. People eligible via random testing

Since there are a fixed number of daily tests, the people eligible for a test are pooled together based on the priority order. During testing (which happens once daily), people are randomly sampled from this pool and given a test. For instance, consider the Self Reported + Random Testing public health response scenario – self-reported symptomatic individuals are collected in pool one, and those eligible for random testing are collected in pool two. According to the priority order, people are first randomly sampled from pool one and given a test, and only if any tests are left, people are randomly sampled from pool two and tested. We use only RT-PCR tests, which are assumed to have a 100% specificity and 100% sensitivity, thereby ensuring no false positives or false negatives. To account for the time delay in declaring results of RT-PCR tests, [51] we introduce a two-day delay between an individual getting tested and receiving the test result. All positively tested individuals are quarantined in their homes for 14 days to account for the incubation period of COVID-19 [52].

2.3 Simulating the Epidemic

The epidemic is seeded by randomly choosing a set of people and infecting them. The number and location of such seed individuals can be varied to model different scenarios. For example, infecting a large fraction of employees at a particular office mimics a super-spreader event. In our experiments, we choose 100 random seed individuals (on average) in a location-independent manner. A detailed description of this algorithm is given in Appendix S2.

The progress of the disease is represented using disease states: Susceptible, Asymptomatic, Presymptomatic, Mildly Infected, Severely Infected, Recovered, Hospitalised, and Dead. Individuals can be in any one of these disease states, and the transition between different states is shown in Fig. 1. Mathematically, such a system is described by a set of eight coupled ordinary non-linear differential equations given in Appendix S2. A variable of the form λ_{DS}, (where DS is the disease state) refers to the rate at

which an agent exits that corresponding state. For example, λ_A is the constant rate at which an agent exits the Asymptomatic state. Note that λ_S, the rate at which a person exits the Susceptible state is not a constant rate and depends on a variety of factors (see Appendix S2 for a detailed description). The other variables - γ, μ, δ and σ - refer to the probability that an individual enters one of the two branched secondary states after exiting the primary state. The subscript i indicates that these variables are age-stratified. For example, for a given age group, γ_i is the probability that an agent becomes Asymptomatic after exiting the Susceptible state. Similarly, 1-γ_i is the probability that the agent becomes Presymptomatic. The values assigned to these variables are given in Appendix S2. We assume that once people recover from the disease, they cannot get reinfected. For a detailed description of the algorithm which governs transitions between different disease states, refer to Appendix S2.

Calculation of Case Fatality Rate (CFR) Case Fatality Rate (CFR) for a cohort of people identified on a given day is calculated as the fraction of people who died out of that cohort. In our model, individuals are identified if they are tested positive or if they die without getting tested (we assume that people can only die due to COVID-19). In the initial days of the epidemic, before testing has started, only dead people are identified, and CFR is effectively 100%. This leads to a very high value of CFR during the initial days and thus we begin calculating CFR only from day 15.

Calculation of $\mathbf{R_t}$ R_t, also known as the effective reproduction number, is an estimator of the number of infections caused by one infected person. During the COVID-19 pandemic, public health systems used R_t to guide and direct public health responses [53]. We use the R Package, EpiEstim [54] to calculate R_t. EpiEstim computes R_t using only daily incidence data and the serial interval distribution – the estimated time between symptom onset in a case and their infector. EpiEstim has been validated against both simulation and public-health data for COVID-19 [54]. For details on the parameters used while computing R_t, please refer to Appendix S7.

Analysis of Contact Tracing Data from Pune Anonymized contact tracing data was used to compute the average number of contacts. The Ethics Committee of Indian Institute of Science Education and Research, Pune, India approved the analysis of

COVID-19 programmatic data.

2.4 Experimental Design

A public health response is a combination of different interventions that can be implemented. The interventions are (a) **Self Reported (SR)** - Only people who self-report are tested, (b) **Contact Tracing (CT)** - Identified high-risk contacts are tested, and low-risk contacts are isolated and (c) **Random Testing (RT)** - people who are randomly sampled from the population are tested.

To compare the relationship between metrics and the true state of the epidemic, we conduct four sets of experiments -

1. Variation of λ_S in the absence of any public health intervention, where λ_S is the rate at which an agent exits the Susceptible state,

2. Variation of the public health response given a fixed number of 500 daily tests. We use the following combinations of interventions

   (a) Self Reported (SR)

   (b) Self Reported along with Contact Tracing (SR+CT)

   (c) Self Reported along with Random Testing (SR+RT)

   (d) Self Reported along with Contact Tracing and Random Testing (SR+RT+CT)

3. Variation of the number of daily tests given a fixed public health response (SR+RT+CT)

4. Variation of the efficiency of contact tracing given a fixed number of 500 daily tests and a fixed public health response - SR + RT + CT. This involves varying two parameters, f_O and f_N which describe the fraction of identified contacts at the office and neighbourhood respectively.

All the values of the described parameters which are varied during each experiment are given in Table 1. Since our model is inherently stochastic in nature, we ran 30 simulations for each set of parameters, and our results are based on an average of these 30 simulations for each parameter set.

Sr.no	Description	Variation of parameters
1	Variation of λ_S	0.3, 0.4, 0.5
2	Variation of public health scenarios given 500 daily tests	• Self Reported • Self Reported + Contact Tracing • Self Reported + Random Testing • Self Reported + Contact Tracing + Random Testing
3	Variation of the number of daily tests given a fixed public health response - Self Reported + Contact Tracing + Random Testing	100,200,300,500,700
4	Variation of efficiency of contact tracing (fraction of contacts identified at office,fraction of contacts identified in the neighborhood) given 500 daily tests and a fixed public health response - Self Reported + Contact Tracing + Random Testing	• **low** - $(0.05, 0.025)$ • **medium** - $(0.15, 0.075)$ • **high** - $(0.25, 0.125)$

Table 1. Description of the parameters varied during each experiment. There are four different public health response scenarios - (1) **SR** Only people who self-report are tested, (2) **SR + CT** People who self-report, identified high-risk contacts and low-risk symptomatic contacts are tested, (3) **SR + RT** People who self-report and people who are randomly tested, (4) **SR + RT + CT** People who self-report, identified high-risk contacts, low-risk symptomatic contacts as well as people who are randomly sampled from the population are tested. Note that there are 40 employees in an office and 400 people in a neighbourhood on average (see **Supplementary Material Section S1.2** so the following fractions translate to 2(10), 6(30), and 10(50) contacts identified at the office (neighbourhood) on average per individual. **SR** - Self Reported, **CT** - Contact Tracing, **RT** - Random Testing

3 Results

3.1 Infection curves for different values of λ_S

We ran simulations for three different λ_S values - $0.3, 0.4$, and 0.5 - in the absence of any public health interventions. A comparison of the infection curves for the three chosen values of λ_S — 0.3, 0.4, and 0.5 is presented in Fig. S4 in Appendix S2. Upon analyzing the results of these simulations, we chose $\lambda_S = 0.5$ for all our further experiments to ensure that around $60 - 70\%$ of the population is infected by the end of the epidemic. We do not analyse these experiments further since it is not in the scope of the current work.

3.2 A comparison between different public health response scenarios given 500 daily tests

We model different public health response scenarios given a fixed number of 500 daily tests. We choose 500 daily tests since this was similar to the maximum number of daily tests (per 100,000 people) that were available in Pune during the second wave (Feb-May 2021) [48]. For the scenarios when contact tracing is active, we set f_O and f_N to be equal to 0.1 and 0.02 respectively which means that on average, 4 colleagues and 8 neighbours are identified as contacts of each positively tested person.

The left column of Fig. 2 shows the evolution of the Test Positivity Rate (TPR) across different public health response scenarios. It is evident that contact tracing effectively reduces the Test Positivity Rate (TPR). Whenever the contact tracing intervention is active, self-reported symptomatic individuals, high-risk contacts, and low-risk symptomatic contacts have an equal priority to get tested. Since the number of daily tests is fixed, a significant fraction of the tests are used on high-risk contacts who are not necessarily infected, and this brings down the TPR. Random testing has no effect on the TPR in the initial days of the epidemic. This is because the number of daily tests available is fixed and given the priority order, there are barely any tests left for random testing. If the number of daily tests is increased, a larger fraction of tests will be used for random testing (see Fig. S15 in Appendix S8) which will lead to a reduction in the TPR. The absence of the random testing intervention has a significant effect on metrics at the end of the epidemic, where a second smaller peak in TPR is observed. During this period, only a tiny fraction of people remain infected, and the pool of people susceptible to COVID-19 but infected by some other flu-like illness also reduces (as the susceptible population reduces). Thus, there is a high chance that a majority of the people getting tested are symptomatic, which in turn increases the TPR. This result suggests that increases in TPR after an observed epidemic peak declines [19] may be simply due to this reason. When random testing is active, a majority of tests are used for random testing at the end of the epidemic, reducing TPR and mitigating this effect, as shown in the respective panels in Fig. 2. However, we note that this reduction in TPR is purely "cosmetic" in the sense that it has no impact on health outcomes (see Fig. S5 in Appendix S4). Note that our TPR values are significantly higher as compared

to actual reported values in Pune city (see Fig. S12 in Appendix S6). This is because we are only analyzing a population contained within a single hypothetical ward. There is no migration of people between different wards and hence, it is easier to identify and test people with symptoms as well as trace contacts. The right panel of Fig. 2 shows that contact tracing effectively reduces the Case Fatality Rate (CFR).

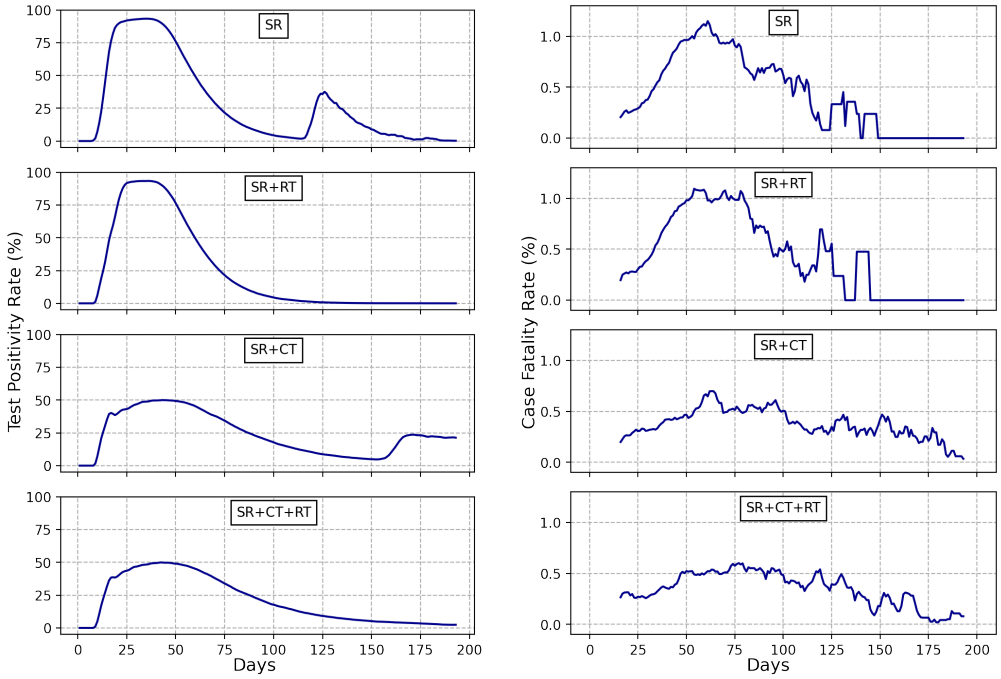

Fig 2. The left and right panels show the evolution of the Test Positivity Rate (TPR) and the Case Fatality Rate (CFR) respectively, for different public health response scenarios given a fixed number of 500 daily tests. The plots show an average of the metrics taken over 30 individual simulation runs. Furthermore, each metric curve is smoothed over using a 7-day rolling average.

The left column of Fig. 3 compares the evolution between the actual number of infected people (or the number of true infections) and TPR. There is an indication of a weak phase relationship as both of these curves rise and fall together. The second peak in TPR for the SR and SR + CT scenarios is due to the absence of random testing as mentioned above. The right panel of Fig. 3 compares the evolution of the rate of change of true infections with the rate of change of TPR. The stars denote the corresponding days on which this rate goes to 0 or the days on which the infection or TPR curves peak. The TPR peaks slightly before the infection for all the public health response scenarios considered. Moreover, for all scenarios, the rate of change of TPR always peaks before

the rate of change of the number of true infections and subsequently the true infection peak (given by the location of the red star). This result suggests that the rate of change in TPR is a promising indicator for the peak of the actual number of infections. In the absence of random testing, the rate of change of TPR shows a small peak at the end of the epidemic which is a manifestation of the second peak in TPR. A similar analysis comparing the evolution of the number of true infections and the Case Fatality Rate (CFR) is shown in Fig. S10 in Appendix S5. For all the public health response scenarios, the CFR peaks after the infection curve and thus, the CFR metric cannot be used to forecast the peak of the infection curve. Nevertheless, the peak of the infection curve occurs between the peak of the rate of change of TPR and the CFR and thus these two metrics together can be used to estimate the state of the epidemic.

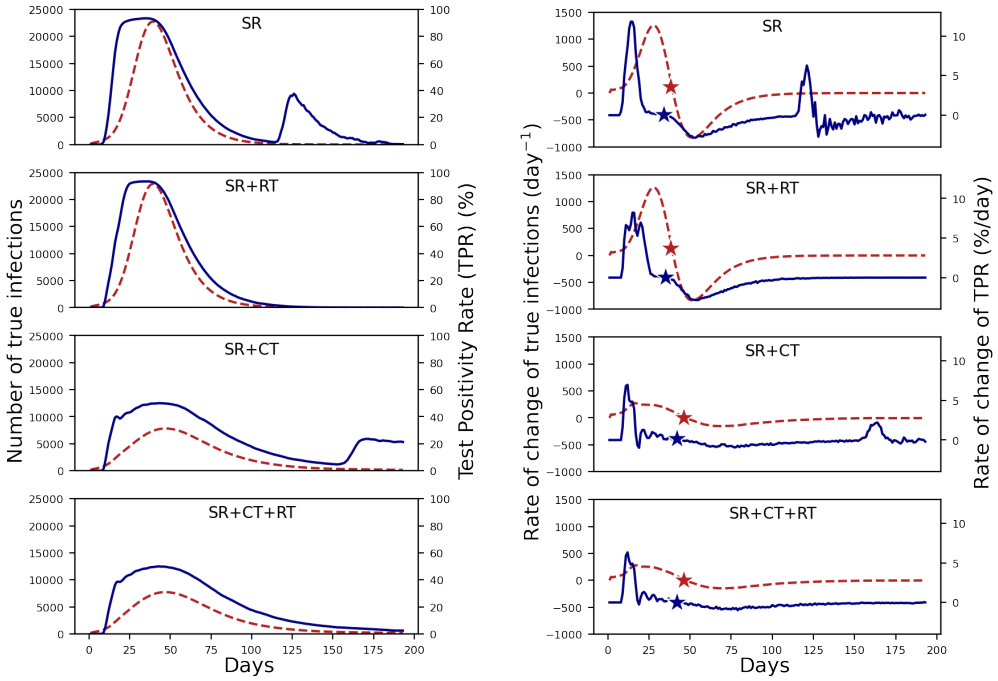

Fig 3. The left panel shows a comparison between the metric TPR (solid blue line) with the number of true infections (dashed red line) for different public health responses. The right panel shows a comparison between the rate of change of metric TPR (solid blue line) with the rate of change of the number of true infections (dashed red line) for different public health responses. The stars denote the days on which the rate of change of true infections or the metric TPR goes to 0 or in other words, the days on which the infection and the TPR curves peak. All the plots correspond to a 7-day rolling average.

3.3 A comparison between different number of daily tests given a fixed public health response (SR+CT+RT).

In this experiment, we vary the number of daily tests given a fixed public health response (SR + RT + CT). f_O and f_N, the fraction of identified contacts at the office and neighbourhood, are set to 0.1 and 0.02 respectively. Fig. S6 in Appendix S4 shows the evolution of the number of true infections and the number of cumulative deaths for different numbers of daily tests. It is observed that the number of true infections and the number of cumulative deaths decrease with an increase in the number of daily tests. However this decrease is not linear as both these quantities saturate after a subsequent increase in the number of daily tests. Fig. 4 depicts the evolution of the Test Positivity Rate (TPR) and the Case Fatality Rate (CFR). Both these metrics show a reduction as the number of daily tests are increased. The TPR reduces simply because as the number of tests are increased, the fraction of positive tests reduces while the reduction in CFR is a consequence of the reduction in the number of deaths. However, this reduction is non-linear in both the cases. Even after a 7-fold increase in the number of tests from 100 to 700, the peak of the TPR only reduces roughly by a factor of half, suggesting that increasing testing with the aim to reduce TPR may not be very effective. As the number of tests increase seven-fold, the peak of the TPR curve drops by $\sim 40\%$ and the peak of the infection curve also drops by roughly the same amount. However, the CFR drops by $\sim 90\%$ while the number of cumulative deaths reduces by $\sim 25\%$. Thus, the change in TPR roughly correlates with the change in the number of true infections but the change in CFR is not reflected proportionally by the change in the number of cumulative deaths.

The left panel of Fig. 5 shows that we observe a consistent phase relationship between TPR and the number of true infections. As shown before, the peak of the rate of change of TPR is seen slightly before the peak of rate of change of number of true infections and much before the peak of the infection curve itself (given by the location of the red star). This again indicates that the rate of change of TPR is an excellent metric for forecasting the peak in the number of true infections. As observed earlier, the peak of the CFR occurs after the peak of the number of true infections (see Fig. S11 in Appendix S5).

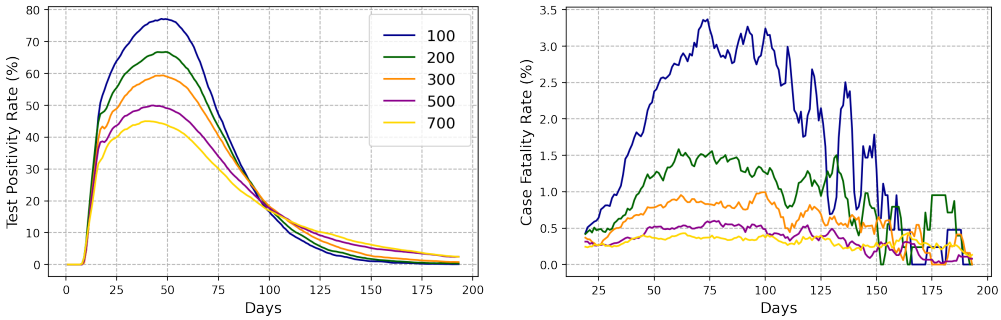

Fig 4. Evolution of the Test Positivity Rate (left) and the Case Fatality Rate (right) for different number of available daily tests, given a fixed public health response - SR + CT + RT. All plots correspond to a 7-day rolling average.

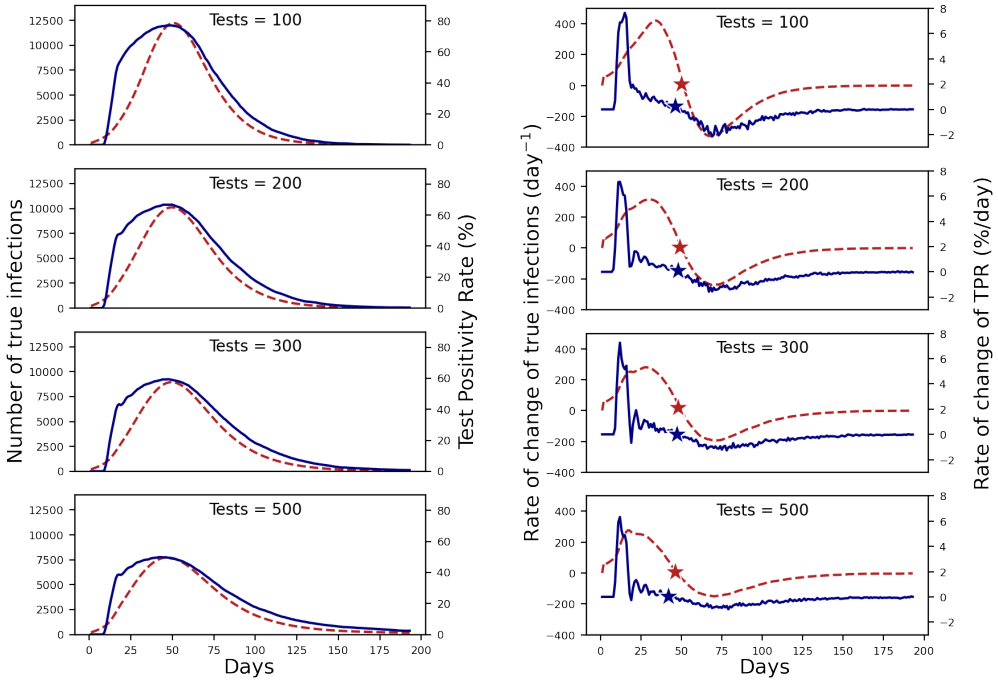

Fig 5. The left panel shows a comparison between the number of true infections (dashed red line) and the TPR (solid blue line) and the right panel compares the rate of change of the number of true infections (dashed red line) with the rate of change of TPR (solid blue line) for different numbers of daily tests given a fixed public health response - SR + RT + CT. The stars denote the days on which the corresponding rates go to 0 or the days on which the infection and the TPR curves peak. All the plots correspond to a 7-day rolling average.

3.4 A comparison between different efficiencies of contact tracing

In this section, we explore the isolated effects of the "efficiency" of contact tracing. We simulate a fixed public health response - SR + CT and vary the values of f_O and f_N - (i)

$(0.05, 0.025)$, (ii) $(0.15, 0.075)$, and (iii) $(0.25, 0.125)$, given a fixed number of 500 daily tests. These respective scenarios are labelled as low, medium and high and these labels characterize the efficiency of contact tracing and thus, the number of contacts identified for each positively tested person. Fig. S7 in Appendix S4 shows the evolution of the number of true infections and the number of cumulative deaths for all three contact tracing efficiencies. Since the infection wave does not end even after 200 days, we extend our simulation time to 400 days.

The left column of Fig. 6 shows that increasing the efficiency of contact tracing reduces the peak of the TPR, but increases the spread of the TPR curve. For example, when the contact tracing efficiency is high, TPR shows a gradual decline and only reduces to about 75% of its maximum value even after 400 days. The reasons for this are twofold; (i) the length of the epidemic itself is extended, and (ii) increasing the efficiency increases the number of identified contacts and a significant fraction of tests are utilized on testing them, leaving a constant symptomatic pool of people within the testing queue who will get tested positive. Thus, in this case, TPR does not capture the dynamics of the epidemic as the TPR curve reflects the positivity of those in the queue rather than the current state of the epidemic curve. The second peak in TPR is due to the absence of random testing, as explained above.

Fig. 6 shows that the reduction in CFR and TPR is not linear with an increase in the efficiency of contact tracing and both metrics exhibits a threshold-like behaviour. This is evident from the fact that increasing the contact tracing efficiency from medium to high has negligible effect on either CFR or TPR. However, the health outcomes do not show a similar trend and are markedly different. As the contact tracing efficiency is increased from low to high, the peak of the infection curve drops by $\sim 70\%$ and the total number of deaths drops by $\sim 35\%$. The metrics do not show a proportionate reduction as the TPR only drops by $\sim 20\%$ and the CFR drops by $\sim 50\%$. Thus its difficult to draw any inferences about the state of the epidemic and health outcomes just from changes in CFR and TPR when the efficiency of contact tracing changes.

Our analysis on the phase relationships yield similar results as earlier (see Fig. 7); the peak of the rate of change of TPR happens much before the peak of the epidemic given by the location of the red star, and thus the rate of change of TPR can forecast the peak of the epidemic.

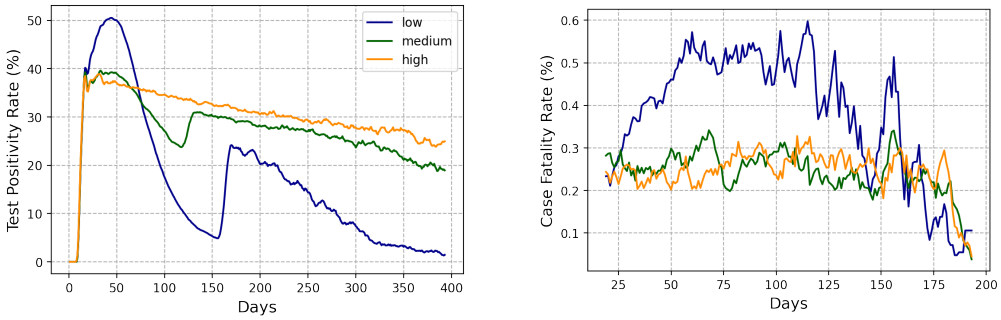

Fig 6. Evolution of the Test Positivity Rate (left) and the Case Fatality Rate (right) for different efficiencies of contact tracing, given a fixed public health response - SR + CT and a fixed number of 500 daily tests. All plots correspond to a 7-day rolling average. Note that the CFR is only plotted till day 200 since it shows a lot of fluctuations in the days beyond that (see Appendix S5).

3.5 Phase relationships when testing is unconstrained by number of tests

In all our experiments described above, it is observed that almost all the available daily tests are used up throughout the duration of the epidemic (see Fig. S16 in Appendix S8). As a result, the number of positive tests and the test positivity rate are always in phase with each other, as the number of positive tests is an integer multiple of the test positivity rate if all available tests are used up (given that each test has a 100% specificity and 100% sensitivity). To compare the phase relationships between different quantities when the test positivity rate is not in phase with the number of positive tests, we explore three scenarios with excessive number of available daily tests - 1500, 2000 and 2500, with SR being the only active public health response. We make these choices to mimic the situation in Pune city during the second wave of COVID-19 (March-May 2021) when testing was not constrained by availability of tests, but contact tracing was no longer conducted due to the very large number of infections. Moreover, to ensure that testing starts early, we increase the number of randomly infected seed individuals to 1000.

Fig. 8 shows that in this scenario, the rise in TPR leads the rise in the number of identified cases. This is due to the fact that a lower fraction of the daily tests get used up when the number of available daily tests is increased (see Fig. S17 in Appendix S8) and the number of positive tests and TPR is no longer in phase. Furthermore, the daily

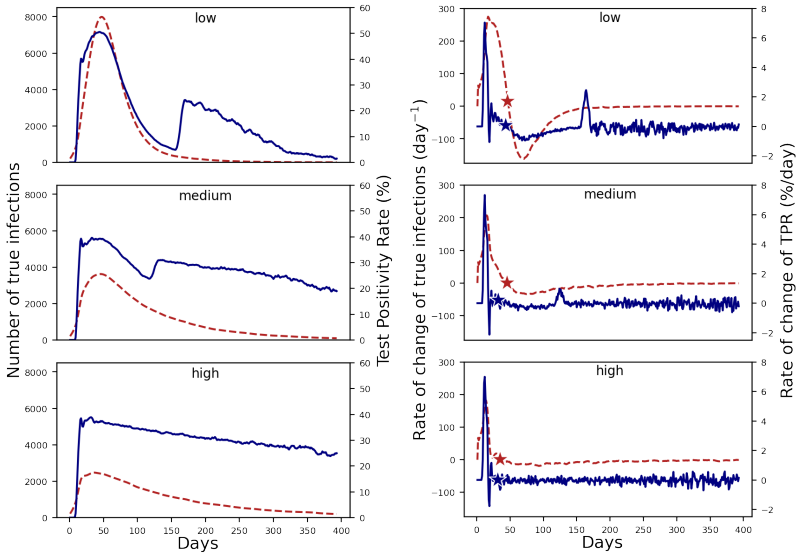

Fig 7. The left panel shows a comparison between the number of true infections given (dashed red line) and the TPR (solid blue line) while the right panel compares the rate of change of number of true infections (dashed red line) with the rate of change of TPR (solid blue line) for different efficiencies of contact response keeping a fixed public health response - SR + CT and a fixed number of 500 daily tests. The stars denote the days on which the infection and the TPR curves peak or the days when the corresponding rates go to 0. All the plots correspond to a 7-day rolling average.

identified cases closely tracks the rise of actual number of cases, which means that the rapidly increasing TPR is a good predictor of increasing number of actual infections. Fig. 8 shows that the number of positive tests peaks before the number of true infections in all three scenarios, making it a good indicator of the peak of the epidemic curve.

For all three scenarios, the TPR is so high because only people with symptoms who self-report are getting tested, so there is no contact tracing or random testing. As described before in subsection 2.2, symptomatic people who self-report are divided into two pools - (i) People who are infected with COVID-19 and (ii) People who are infected with influenza-like illnesses (ILIs) and show similar symptoms but are still susceptible to COVID. The test positivity rate is a reflection of the fraction of people who are tested from each pool. Figure Fig. S18 in Appendix S8 shows a comparison between the number of positive tests versus the number of people with ILIs who are tested for all the three excess test scenarios. For the first case with 1500 tests, the peak of the number of people with ILIs who are tested occurs after the infection peak when the number of positive tests is also on the decline. Thus, during this period, there is a significant

reduction in TPR as a modest fraction of the testing pool is made up of people with ILIs. However, as sufficient tests become available during the decline of the epidemic, a majority of persons with ILIs are tested at the same time and they rapidly fall out of the testing pool. Thus, TPR starts rising again producing a second peak in the TPR curve. This is similar to the second peak in TPR produced in the absence of random testing (see subsection 3.2). As the number of tests is increased to 2000, the number of tested people with ILIs is almost in-phase with the number of positive tests and again falls rapidly after the peak. Thus we see a smaller dip in the TPR curve. For the case with the highest number of tests, the two quantities are exactly in phase with each other and thus TPR does not show a dip and a subsequent second peak.

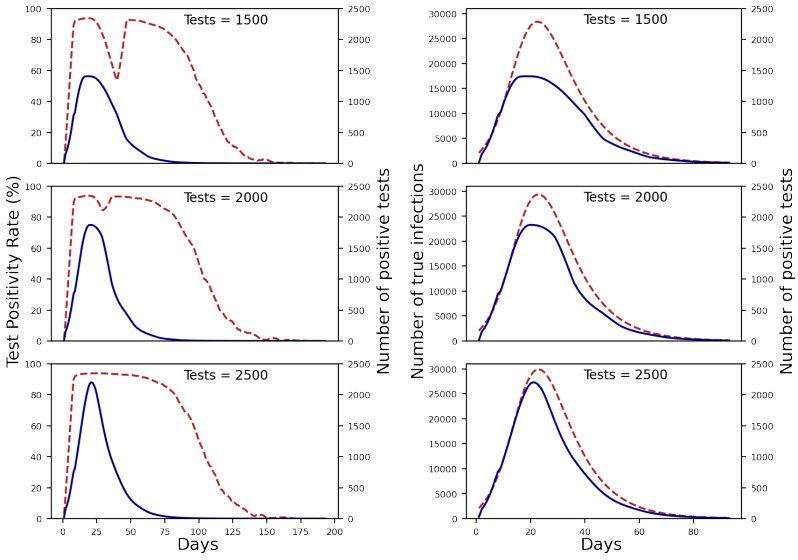

Fig 8. The left panel shows a comparison of the relationship between the Test Positivity Rate (dashed red line) and the number of positive tests (solid blue line). The right panel compares the number of true infections (dashed red line) with the number of positive tests (solid blue line) for different numbers of daily tests given a fixed public health response - SR.

3.6 A comparison of phase relationships between R_t and the epidemic

Effective Reproduction Number, or R_t has been used by several public health systems to judge the state of the epidemic and guide public health response. To examine the fidelity of R_t estimated using surveillance data in capturing the growth and decay phase

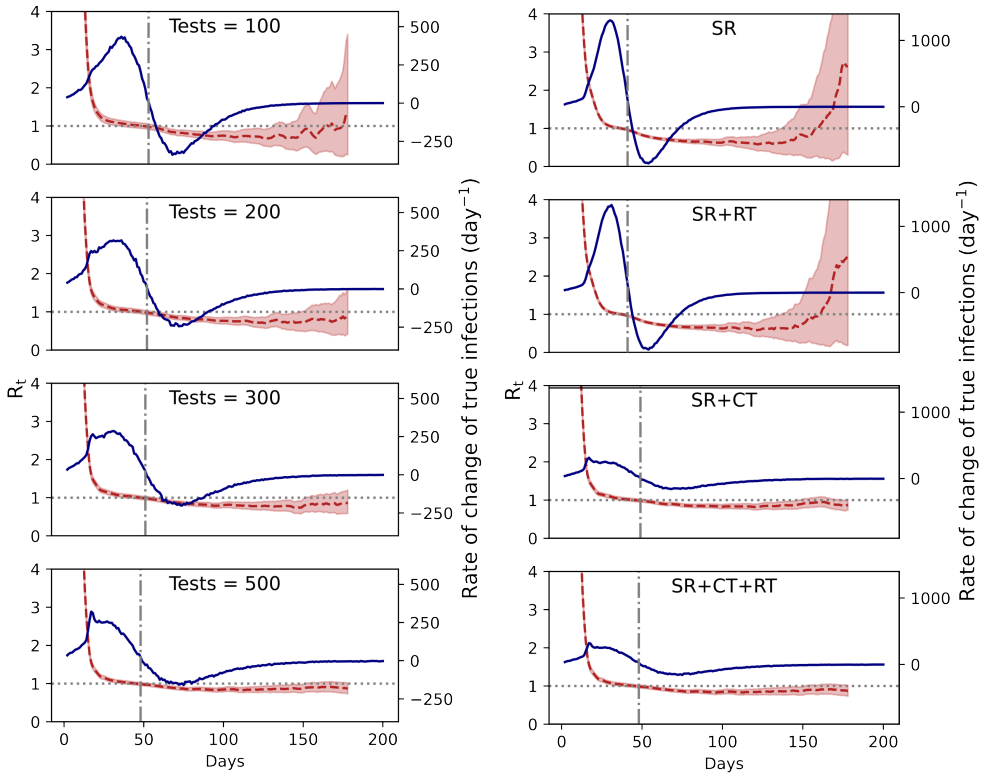

Fig 9. Plot showing the relationship between R_t (dashed red line) and the rate of change of true infections per day (solid blue line) for (left) different number of daily tests and (right) different public health scenarios. The shaded red regions around the dashed lines depict the 90% confidence intervals of R_t. The horizontal grey dotted line indicates $R_t = 1$. The vertical dotted grey line indicates the peak of true infections.

of the epidemic, we plot R_t estimated using EpiEstim against number of infections. The value of R_t is expected to indicate whether the epidemic is post its peak. We find that in all scenarios (Fig. 9), R_t dips below 1 just before the infection peak. This is true even in cases where positive cases and infected are not in phase (see Appendix S7). We note that in cases where contact tracing is not active, R_t produces a secondary peak close to the end of the epidemic (albeit with large uncertainty), which might indicate the beginning of another wave. Thus, caution must be employed while using the value of R_t, particularly at the end of an epidemic wave when contact tracing was not employed. Furthermore, the estimates of R_t when contact tracing is active are more precise and have much smaller confidence intervals even at the end of the epidemic when very few cases are present.

4 Discussion and conclusion

Public health decision making during an epidemic is based on data obtained from surveillance. The sucess of such decisions in controlling health outcomes relies on the fidelity of the surveillance data in representing the actual epidemic, especially when a majority of the cases go unidentified. While metrics derived from surveillance data such as TPR and CFR have been used [14–16] during the recent COVID-19 epidemic, their actual utility has not been tested in a systematic manner. Thus, the main goal of our work was to use agent-based modelling as a principled approach to both designing and testing such metrics. Put in another way, our work aimed to "construct" the behavior and relationships between different metrics such as TPR and CFR over an epidemic wave and examine how different public health responses lead to different behaviors of such metrics. This constructivist approach allows for a more nuanced use and interpretation of such metrics.

For instance, our results show that regardless of the type of public health response being active, a TPR-threshold based intervention will be activated too late (if curbing the rise of infections is the aim), and the rate of change of TPR better captures the growth phase of the epidemic in all scenarios that we examined. In extreme cases such as Fig. 8 and Fig. 9, a threshold based approach may keep the intervention active for much longer than is necessary to control infection spread, leading to inefficiencies in usage of scarce resources and unnecessary loss of economic output (in case lockdowns are used). Furthermore, the peak rate of change of TPR occurs just before the epidemic itself peaks, providing a way to estimate future requirements for healthcare infrastructure. Our results also show that CFR tends to peak when the epidemic is already on the decline – even if CFR is assigned based on the date of identification of the infected person rather than date of death – and in some cases has no clear peak at all, making it problematic as a metric for decision making. Our results suggest that R_t is also a reliable metric in predicting the epidemic peak, but may falsely indicate a rise in infections (i.e, a second wave) at the end of the epidemic wave. Thus, confidence intervals associated with the estimated R_t must be taken into account at all times.

Our results suggest that using such metrics as a way to compare between cities or administrative wards is again problematic since different places may adopt different

public health responses and with different efficiencies. Indeed, better contact tracing leads to higher mean TPR in our simulations which may lead to the false impression that the epidemic is more prevalent or that current contact tracing efficiency is poor. Furthermore, metrics such as TPR and CFR do not scale linearly with the number of true infections or deaths and thus care must be taken while utilizing TPR or CFR to make inferences about likely health outcomes.

While we present an extensive set of public health scenarios, we do not expect our results to be directly applicable to all real world scenarios. One of the main limitations is that we consider an isolated population with no import/export of infections from external sources. This makes the public health response unusually efficient in identifying infections and leads to very high values of TPR. We also speculate that this may be one of the reasons why we are unable to simulate the phase difference between the number of identified infections and metrics such as TPR. Furthermore, we do not account for differential delays in testing, test sensitivity and specificity, reinfections, and transmission through non-airborne medium. We also do not account for pharmaceutical interventions such as medicines, vaccines and antibody therapy and non-pharmaceutical interventions such as lock downs. However, the aim of our work was to develop a principled approach to constructing observed epidemic curves, and thus such enhancements are left to future work.

Our results show potential to assist public health professionals in decision making during future epidemics. Through extensive simulations of epidemics and public health responses, we provide modelling evidence to support the use of some metrics for decision making.

5 Acknowledgements

PB acknowledges the Department of Science and Technology, Government of India for the KVPY fellowship.

SK acknowledges the Department of Science and Technology, Government of India for the INSPIRE fellowship.

PC acknowledges support from Ashoka University and the Mphasis F1 Foundation and would like to thank Gautam Menon, Vaibhhav Sinha, and Riz Noronha for many

useful discussions.

The authors acknowledge the support and the resources provided by PARAM Brahma Facility under the National Supercomputing Mission, Government of India at the Indian Institute of Science Education and Research, Pune.

The authors thank Ashwini Keskar and Pune Knowledge Cluster for providing the daily epidemiological surveillance data from Pune.

The authors would also like to thank the BharatSim team at ThoughtWorks and Ashoka University, with special thanks to Jayanta Kshirsagar and Gaurav Deshkar from the ThoughtWorks Engineering for Research team for many discussions regarding the use and optimisation of BharatSim.

References

1. Institute of Medicine (US) Forum on Emerging Infections. Public Health Systems and Emerging Infections: Assessing the Capabilities of the Public and Private Sectors: Workshop Summary. Washington (DC):. National Academies Press (US); 2000.Available from: http://www.ncbi.nlm.nih.gov/books/NBK100253/.

2. COVID-19 in Pune | DSCMS, PKC;. Available from: http://cms.unipune.ac.in/~bspujari/Covid19/Pune2/.

3. Sujath R, Chatterjee JM, Hassanien AE. A machine learning forecasting model for COVID-19 pandemic in India. Stochastic Environmental Research and Risk Assessment. 2020;34:959–972.

4. Shastri S, Singh K, Kumar S, Kour P, Mansotra V. Time series forecasting of Covid-19 using deep learning models: India-USA comparative case study. Chaos, Solitons & Fractals. 2020;140:110227.

5. Gupta R, Pal SK. Trend Analysis and Forecasting of COVID-19 outbreak in India. MedRxiv. 2020; p. 2020–03.

6. Dash S, Chakraborty C, Giri SK, Pani SK, Frnda J. BIFM: Big-data driven intelligent forecasting model for COVID-19. IEEE Access. 2021;9:97505–97517.

7. Sarkar K, Khajanchi S, Nieto JJ. Modeling and forecasting the COVID-19 pandemic in India. Chaos, Solitons & Fractals. 2020;139:110049.

8. Agrawal S, Bhandari S, Bhattacharjee A, *et al* . City-scale agent-based simulators for the study of non-pharmaceutical interventions in the context of the COVID-19 epidemic. Journal of the Indian Institute of Science 2020;**100**:809–47.

9. Cherian P, Kshirsagar J, Neekhra B, Deshkar G, Hayatnagarkar H, Kapoor K, et al. BharatSim: An agent-based modelling framework for India. medRxiv. 2023; p. 2023–06.

10. Shinde GR, Kalamkar AB, Mahalle PN, Dey N, Chaki J, Hassanien AE. Forecasting models for coronavirus disease (COVID-19): a survey of the state-of-the-art. SN Computer Science. 2020;1:1–15.

11. Bertozzi AL, Franco E, Mohler G, Short MB, Sledge D. The challenges of modeling and forecasting the spread of COVID-19. Proceedings of the National Academy of Sciences. 2020;117(29):16732–16738.

12. Ioannidis JP, Cripps S, Tanner MA. Forecasting for COVID-19 has failed. International journal of forecasting. 2022;38(2):423–438.

13. Parag KV, Donnelly CA, Zarebski AE. Quantifying the information in noisy epidemic curves. Nature Computational Science. 2022;2(9):584–594.

14. WHO. Public health criteria to adjust public health and social measures in the context of COVID-19: annex to considerations in adjusting public health and social measures in the context of COVID-19, 12 May 2020. World Health Organization; 2020.

15. Gupta N, Rana S, Panda S, Bhargava B. Use of COVID-19 test positivity rate, epidemiological, and clinical tools for guiding targeted public health interventions. Frontiers in Public Health. 2022;10.

16. Vaman RS, Valamparampil MJ, Augustine AE. Using Test Positivity Rate (TPR) as an Indicator for Strategic Action in COVID-19: A Situational Analysis in Kerala, India. Indian Journal of Clinical Medicine. 2020;10(1-2):31–35.

17. Express Web Desk. Covid-19 lockdown: Centre identifies red, orange, green zones for week after May 3; check full list here; 2020. https://indianexpress.com/article/india/covid-19-lockdown-centre-identifies-red-green-orange-zones-for-week-after-may-3-check-full-list-here-6388654/.

18. Times of India. Coronavirus: Centre issues state-wise division of red, orange, green zones; 2020. https://timesofindia.indiatimes.com/india/coronavirus-health-ministry-designates-districts-into-red-orange-green-zones/articleshow/75484756.cms.

19. Namrata Devikar. After Centre's nudge, health dept to increase testing in Maharashtra. Hindustan Times. 2022;.

20. Monteiro J, Pujari B, Bhattacharrya SM, Raghunathan A, Keskar A, Shaikh A, et al. Into the thirteenth Month: A Case Study on the Outbreak Analytics and Modeling the spread of SARS-CoV-2 Infection in Pune City, India. medRxiv. 2021; p. 2021–06.

21. Carter P, Megnin-Viggars O, Rubin GJ. What factors influence symptom reporting and access to healthcare during an emerging infectious disease outbreak? A rapid review of the evidence. Health security. 2021;19(4):353–363.

22. Biswas RK, Afiaz A, Huq S. Underreporting COVID-19: the curious case of the Indian subcontinent. Epidemiology & Infection. 2020;148:e207.

23. Alvarez E, Bielska IA, Hopkins S, Belal AA, Goldstein DM, Slick J, et al. Limitations of COVID-19 testing and case data for evidence-informed health policy and practice. Health Research Policy and Systems. 2023;21(1):11.

24. George CE, Inbaraj LR, Chandrasingh S, de Witte LP. High seroprevalence of COVID-19 infection in a large slum in South India; what does it tell us about managing a pandemic and beyond? Epidemiology & Infection. 2021;149:e39. doi:10.1017/S0950268821000273.

25. Mukherjee B, Purkayashtha S, Kundu R, Bhaduri R. Estimating the Infection Fatality Rate from SARS-CoV-2 in India. SSRN Electronic Journal. 2021;doi:10.2139/SSRN.3798552.

26. Cherian P, Krishna S, Menon GI. Optimizing testing for COVID-19 in India. PLOS Computational Biology. 2021;17:e1009126. doi:10.1371/JOURNAL.PCBI.1009126.

27. Gomez J, Prieto J, Leon E, Rodríguez A. INFEKTA—An agent-based model for transmission of infectious diseases: The COVID-19 case in Bogotá, Colombia. PloS one. 2021;16(2):e0245787.

28. Hazra DK, Pujari BS, Shekatkar SM, Mozaffer F, Sinha S, Guttal V, et al. The INDSCI-SIM model for COVID-19 in India. medRxiv. 2021; p. 2021–06.

29. Mozaffer F, Cherian P, Krishna S, Wahl B, Menon GI. Effect of hybrid immunity, school reopening, and the Omicron variant on the trajectory of the COVID-19 epidemic in India: a modelling study. The Lancet Regional Health-Southeast Asia. 2023;8:100095.

30. Singh A, Arquam M. Epidemiological modeling for COVID-19 spread in India with the effect of testing. Physica A: Statistical Mechanics and its Applications. 2022;592:126774.

31. Kerr CC, Stuart RM, Mistry D, Abeysuriya RG, Rosenfeld K, Hart GR, et al. Covasim: an agent-based model of COVID-19 dynamics and interventions. PLOS Computational Biology. 2021;17(7):e1009149.

32. CESSI. CESSI COVID-19 Dashboard;. Available from: http://www.cessi.in/coronavirus/.

33. Mave V, Shaikh A, Monteiro JM, Bogam P, Pujari BS, Gupte N. Association of National and Regional Lockdowns with COVID-19 Infection Rates in Pune, India. Scientific Reports. 2022;12(1):10446. doi:10.1038/s41598-022-14674-0.

34. Ghose A, Bhattacharya S, Karthikeyan AS, Kudale A, Monteiro JM, Joshi A, et al. Community Prevalence of Antibodies to SARS-CoV-2 and Correlates of Protective Immunity in Five Localities in an Indian Metropolitan City. medRxiv. 2020; p. 2020.11.17.20228155. doi:10.1101/2020.11.17.20228155.

35. Bogam P, Joshi A, Nagarkar S, Jain D, Gupte N, Shashidhara L, et al. Burden of COVID-19 and case fatality rate in Pune, India: an analysis of

the first and second wave of the pandemic. IJID Regions. 2022;2:74–81. doi:10.1016/J.IJREGI.2021.12.006.

36. Hazra DK, Pujari BS, Shekatkar SM, Mozaffer F, Sinha S, Guttal V, et al. Modelling the first wave of COVID-19 in India. PLoS computational biology. 2022;18(10):e1010632.

37. Govt of Maharashtra. Levels of Restriction for Breaking the Chain; 2021.

38. The Indian Express. Pune City, Rural Areas May See Covid Restrictions Easing as Test Positivity Rate Comes down — Pune News; 2021. https://indianexpress.com/article/cities/pune/pune-city-rural-areas-covid-restrictions-test-positivity-rate-7352596/.

39. DNA. Maharashtra Unlock 2.0: 5-Level Unlock Plan Begins, Check What's Allowed in Your District; 2021. https://www.dnaindia.com/india/report-maharashtra-5-level-unlock-plan-begins-today-mumbai-local-trains-restaurants-malls-whats-allowed-full-list-of-guidelines-cm-uddhav-thackeray-2893923.

40. Chiu WA, Ndeffo-Mbah ML. Using Test Positivity and Reported Case Rates to Estimate State-Level COVID-19 Prevalence and Seroprevalence in the United States. PLOS Computational Biology. 2021;17(9):e1009374. doi:10.1371/journal.pcbi.1009374.

41. Chiu WA, Ndeffo-Mbah ML. Calibrating COVID-19 Community Transmission Risk Levels to Reflect Infection Prevalence. Epidemics. 2022;41:100646. doi:10.1016/j.epidem.2022.100646.

42. Wiegand RE, Deng Y, Deng X, Lee A, Meyer WA, Letovsky S, et al. Estimated SARS-CoV-2 Antibody Seroprevalence Trends and Relationship to Reported Case Prevalence from a Repeated, Cross-Sectional Study in the 50 States and the District of Columbia, United States—October 25, 2020–February 26, 2022. The Lancet Regional Health - Americas. 2023;18:100403. doi:10.1016/j.lana.2022.100403.

43. Toh KB, Runge M, Richardson RA, Hladish TJ, Gerardin J. Design of Effective Outpatient Sentinel Surveillance for COVID-19 Decision-Making: A Modeling Study; 2022.

44. National Centre for Disease Informatics and Research. Three-Year Report of Population Based Cancer Registries 2012-2014; 2016. https://ncdirindia.org/All_Reports/PBCR_REPORT_2012_2014/ALL_CONTENT/Printed_Version.html.

45. Andrews M, Areekal B, Rajesh K, Krishnan J, Suryakala R, Krishnan B, et al. First confirmed case of COVID-19 infection in India: A case report. The Indian journal of medical research. 2020;151(5):490.

46. Thakur S, Chauhan V, Galwankar S, Kelkar D, Vedhagiri K, Aggarwal P, et al. Covid-19 testing strategy of India–Current status and the way forward. Journal of Global Infectious Diseases. 2020;12(2):44.

47. Jayaram A, Jagadesh A, Kumar AMV, Davtyan H, Thekkur P, Vilas VJDR, et al. Trends in influenza infections in Three States of India from 2015-2021: Has there been a change during COVID-19 pandemic? Trop Med Infect Dis. 2022;7(6):110.

48. Mascarenhas A. At 12,000, Pune district records highest average daily Covid testing in state. The Indian Express. 2020;.

49. Ritchie H, Mathieu E, Rodés-Guirao L, Appel C, Giattino C, Ortiz-Ospina E, et al. Coronavirus pandemic (COVID-19). Our world in data. 2020;.

50. Indian Council of Medical Research. Advisory on Strategy for COVID-19 Testing in India; 2020.

51. Bedi A. 'Results of 18 Nov RT-PCR tests awaited' — Covid surge sees delays, Delhi officials blame labs; 2020. https://theprint.in/health/results-of-18-nov-rt-pcr-tests-awaited-covid-surge-sees-delays-delhi-offi554510/.

52. Lauer SA, Grantz KH, Bi Q, Jones FK, Zheng Q, Meredith HR, et al. The incubation period of coronavirus disease 2019 (COVID-19) from publicly reported confirmed cases: estimation and application. Annals of internal medicine. 2020;172(9):577–582.

53. Gostic KM, McGough L, Baskerville EB, Abbott S, Joshi K, Tedijanto C, et al. Practical considerations for measuring the effective reproductive number, R t. PLoS computational biology. 2020;16(12):e1008409.

54. Nash RK, Bhatt S, Cori A, Nouvellet P. Estimating the epidemic reproduction number from temporally aggregated incidence data: A statistical modelling approach and software tool. PLOS Computational Biology. 2023;19(8):1–14. doi:10.1371/journal.pcbi.1011439.

Supporting Information

Appendix S1 Description of Agent Based Network Model A description of agents, schedules and locations in our agent based network model

Appendix S2 Epidemic Simulation Details A description of the compartmental model and choice of parameters in our epidemic simulations.

Appendix S3 Public Health Response Simulation Details Information on our public health simulations, including when testing starts.

Appendix S4 Epidemic Outcomes of different experiments Epidemic outcomes of different experiments including data on infections and deaths.

Appendix S5 Evaluation of CFR as a forecast metric Plots of Case Fatality Rate (CFR) against epidemic outcomes to examine its utility as a forecast metric of the epidemic peak.

Appendix S6 Analysis of Public Health Data from Pune Analysis of contact tracing and epidemic metric data from Pune city.

Appendix S7 R_t Analysis Details Details of EpiEstim analysis and plots of R_t against infections for variation of contact tracing and excess tests.

Appendix S8 Distribution of tests Plots of the fraction of tests used up for different scenarios.